Hindawi Publishing Corporation
Advances in Materials Science and Engineering
Volume 2014, Article ID 432031, 8 pages
http://dx.doi.org/10.1155/2014/432031

Research Article

Influence of Molybdenum Content and MoO_x^{y-} Species on the Textural and Structural ZrO_2 Properties

Alberto Hernández Zapién,[1] Juan Manuel Hernández Enríquez,[1] Ricardo García Alamilla,[1] Guillermo Sandoval Robles,[1] Ulises Páramo García,[1] and Luz Arcelia García Serrano[2]

[1]*Instituto Tecnológico de Ciudad Madero, División de Estudios de Posgrado e Investigación, Juventino Rosas y Jesús Urueta s/n, Colonia Los Mangos, 89440 Ciudad Madero, TAMPS, Mexico*
[2]*Centro Interdisciplinario de Investigaciones y Estudios sobre Medio Ambiente y Desarrollo, 30 de Junio No. 1520, Barrio La Laguna Ticomán, 07340 México, DF, Mexico*

Correspondence should be addressed to Juan Manuel Hernández Enríquez; jmanuelher@hotmail.com

Received 4 October 2014; Accepted 28 November 2014; Published 18 December 2014

Academic Editor: Bin Li

The present work proposes to study the incorporation of molybdenum into the zirconium oxide precursor ($Zr(OH)_4$), in order to analyze its possible repercussions on the textural and structural zirconia properties (ZrO_2). For this, the $Zr(OH)_4$ was synthesized by the sol-gel method and modified with 5, 10, and 15 wt% of molybdenum into the stabilized oxide. The synthesized materials were dried at 120°C for 24 h and then were calcined at 600°C for 3 h. The characterization of the solids was carried out by thermal analysis, X-ray diffraction, nitrogen physisorption, infrared spectroscopy, and scanning electron microscopy. The thermal analyses results showed that the change from the amorphous to the crystalline phase of ZrO_2 is shifted to higher temperatures due to the presence of molybdenum content. Tetragonal phase was identified for all synthesized materials, showing a decrease in crystallinity as a function of the metal content. The textural properties were improved due to the incorporation of molybdenum into the ZrO_2 structure, developing specific surface areas which are above up to four times the area of pure ZrO_2. The synthesized materials presented spherical morphology with particle sizes less than 1 μm, with a change of this morphology for high metal contents (15 wt%) being observed.

1. Introduction

Catalysis is a crucial science for the chemical industry development. About 80% of manufactured chemicals are obtained by processes that require the use of a catalyst [1]. Specifically, in the oil refining industry, in processes such as isomerization and alkylation of light paraffins, which involve solid-gas reactions, require solid acid catalysts with adequate specific surface area and high thermal stability [2–5], which may be improved by manipulating some variables during the precursor synthesis. Zirconium oxide (ZrO_2) has been widely studied for this type of reactions because of its acid-base properties [6–9]. This catalytic support can be synthesized via precipitation, microemulsion, hydrothermal synthesis, supercritical synthesis, pyrolysis, microwave, and the sol-gel route [10–12]. The sol-gel method has gained great diffusion since it allows preparing materials with high purity, homogeneity, and controlled final properties [13, 14]. The precursor of zirconium oxide ($Zr(OH)_4$) can be obtained through the sol-gel method using metallic alkoxides, showing high specific surface area after being synthesized; however this parameter decreases by effect of thermal treatments to which the material is subjected for obtaining the stabilized oxide [15, 16] and this evinces its poor thermal stability. In the literature it has been reported that the stability and the specific surface area of zirconium oxide are enhanced by the addition of some promoter agents in its structure (SO_4^{2-}, PO_4^{3-} and BO_3^{3-} ions), which also stabilize the tetragonal phase of ZrO_2 and improve their acidic properties [2, 17–19]. However, the main disadvantage that arises when using

SO_4^{2-} and BO_3^{3-} ions as modifiers of ZrO_2 structure is the susceptibility to evacuation from the material surface when it is subjected to high thermal treatments ($T > 600^{\circ}C$), which leads to a decrease in the specific surface area and a possible change of the crystalline structure [20–22]. Reddy et al. [20] have reported that the addition of Al_2O_3 also acts as a stabilizer of the phase previously cited. The same effect has been observed in the ZrO_2 with the addition of certain metal oxides such as La_2O_3, CeO_2, Y_2O_3, Yb_2O_3, and CaO; however, these materials confer certain basic properties [23–25]. Although it has been observed that the incorporation of these stabilizing agents improves the textural and structural properties of the material, high weight percentages have a negative impact on them [26].

With the aim of improving the textural and structural properties of zirconia and trying to avoid the problems associated with loss of doping agent during thermal treatment of the material, this work proposes the incorporation of molybdenum into the structure of zirconium oxide in the form of molybdate species (MoO_x^{y-}), synthesizing the material by the sol-gel method and varying the metallic charge in the oxide synthesized in 5, 10, and 15 wt%.

2. Materials and Methods

2.1. Synthesis of ZrO_2. The synthesis of zirconium oxide was carried out using the sol-gel method. A solution of zirconium *n*-butoxide, 80 wt%, in 1-butanol was subjected to constant agitation and reflux at 65°C for 1 h. The step of hydrolysis is subsequently completed by slowly adding water/1-butanol solution dropwise. The condensation of the resulting gel was carried out keeping the system for 2 h under the same conditions of synthesis. The material obtained was aged at room temperature for 72 h and dried at 100°C for 24 h, obtaining the precursor hydroxide ($Zr(OH)_4$). The heat treatment of the material was performed at a calcining furnace at 600°C for 3 h.

2.2. Synthesis of MoO_x^{y-}/ZrO_2. Once synthesized, the zirconium hydroxide is proceeded to impregnate it with an ammonium heptamolybdate solution by the incipient wetness technique, attempting to deposit metal loadings in the stabilized oxide of 5, 10, and 15 wt% of molybdenum. Impregnated hydroxides were dried at 100°C for 24 h and calcined in air dynamic atmosphere for 3 h at 600°C. The nomenclature of the synthesized materials is based on the load of the deposited metal, being as follows: 5%Mo/ZrO_2, 10%Mo/ZrO_2, and 15%Mo/ZrO_2.

2.3. Characterization Materials. Synthesized materials were characterized by thermogravimetry, X-ray diffraction, nitrogen physisorption, infrared spectroscopy, and scanning electron microscopy. Thermal analyses were performed on a TA Instruments Thermogravimetric Balance STD2960 Simultaneous DSC-TGA, using an extra dry air flow rate of 10 mL/min and a heating rate of 10°C/min. The diffraction patterns were obtained in an X-ray Bruker Advance D800 diffractometer which used CuKα radiation ($\lambda = 1.5406$ Å) and a graphite monochromator in the secondary beam; the intensities of the diffraction lines were obtained in the range of 0–70° in 2-theta scale, with steps of 0.02° and 2.4 s per point. Infrared spectroscopy was carried out in a Fourier Transform Spectrometer (Perking-Elmer Spectrum One) with transparent wafers containing the sample to be analyzed and KBr as a binder; spectra were recorded at a resolution of 4 cm^{-1} and by coadding 16 scans. The textural characterization of the solids was determined in an Automatic Micromeritics ASAP2405NV1.03 of 6 channels and to determine the morphology of the materials a scanning electron microscope JEOL, model JSM-6390LV, at 30 KV coupled to an X-ray detector was employed.

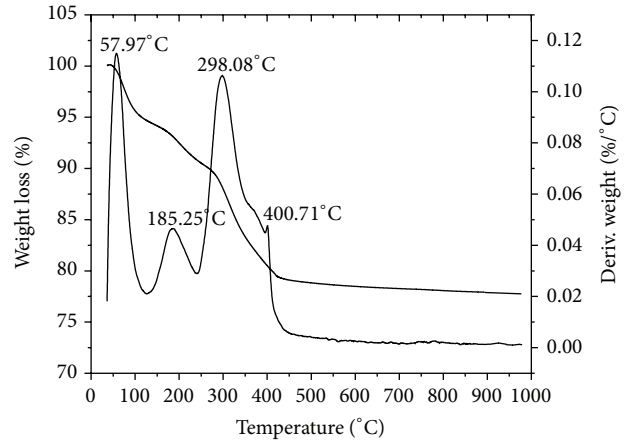

Figure 1: TGA and DTG profiles of $Zr(OH)_4$.

3. Results and Discussion

3.1. Thermal Analysis. Figure 1 shows the TG profile of the synthesized zirconium hydroxide, with three significant weight losses being observed: the first two localized in the range from room temperature to 200°C associated with the evacuation of surface water and alcohol used during the synthesis as well as with the water occluded in the porous structure of the material; these weight losses are related to the exits located on the DTG curve at 60 and 85°C and to the endothermic signals located on the DTA profile at 75 and 190°C (Figure 2) [27]. The third weight loss occurs in the range of 250–450°C and involves two different processes, the first one attributed to the combustion of organic compounds observed at 298°C on the DTG curve and associated with endothermic signals appearing on the DTA profile at 276 and 301°C; the second process located on the DTA curve at 421°C is related to the dehydroxylation of the material as well as the phase transformation of zirconium hydroxide from an amorphous state to a crystalline phase [16, 28].

Thermogravimetric analysis of pure and modified zirconium hydroxide with molybdenum can be seen in Figure 3. This figure shows that in the range from room temperature to 700°C the modified materials have a lower weight loss compared to the unmodified material; this could be related to an exchange of OH– groups by MoO_x^{y-} species verified

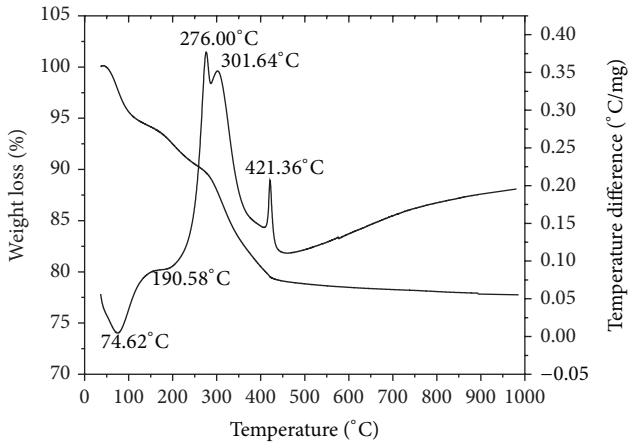

Figure 2: TGA and DTA profiles of $Zr(OH)_4$.

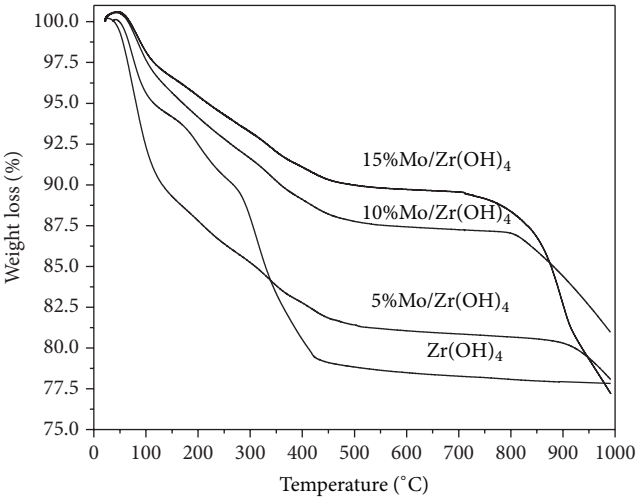

Figure 3: TGA profiles of $Zr(OH)_4$ and $MoO_x{}^{y-}/Zr(OH)_4$.

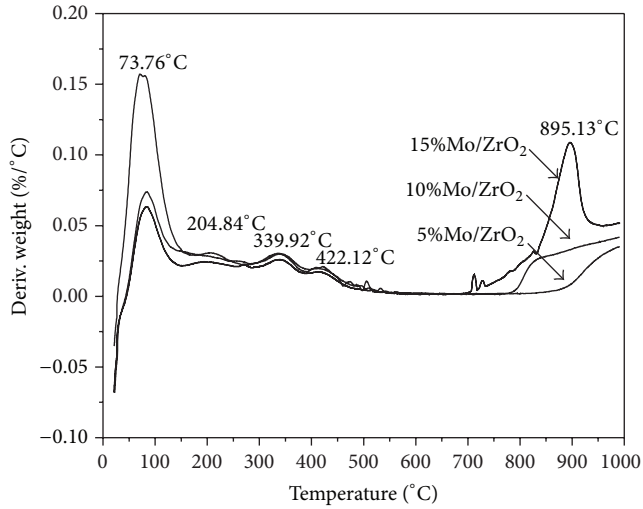

Figure 4: DTG profiles of $Zr(OH)_4$ and $MoO_x{}^{y-}/Zr(OH)_4$.

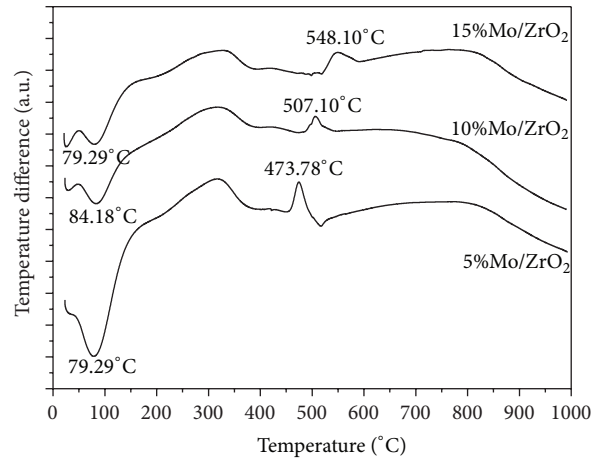

Figure 5: DTA profiles of $MoO_x{}^{y-}/Zr(OH)_4$.

during the zirconium hydroxide step impregnation; these species attached to the zirconium oxide structure improve its stability. For the modified materials an additional weight loss occurs from 700 to 1000°C that could be related to the volatilization of molybdenum and its respective abandonments from the zirconium oxide structure due to the fact that the molybdenum has a vapor pressure of 40 mmHg at 892°C [29, 30] and this weight loss is increased depending on the metal content in the support and is associated with the exits of matter located at around 900°C in the DTG curves reported in Figure 4.

The modified materials with molybdenum have a similar behavior compared to pure zirconium hydroxide in the differential thermal analysis in the range from room temperature to 400°C (Figure 5) and the major difference resides in the signal attributed to the possible change of crystalline phase; this exothermic peak occurs at about 420°C for the unmodified material (Figure 2) but is shifted a higher temperatures due to the presence and content of molybdenum, results that are consistent with those reported by Sohn et al. [31]. In the case of the modified materials, the exothermic peak shows on the DTA curves up at 450°C under the same heating conditions. So far, it appears that the molybdate species ($MoO_x{}^{y-}$) retard the phase transformation process due to the interaction between these species and the zirconium oxide surface causing differences in the observed exotherms. There is no weight loss during the phase transformation process (Figure 3).

3.2. X-Ray Diffraction. The X-ray diffraction patterns of pure and modified zirconium oxide are presented in Figure 6. Usually zirconium oxide as support involves three crystalline phases: monoclinic, tetragonal, and cubic. The zirconium oxides obtained by calcining pure and modified $Zr(OH)_4$ at 600°C during 3 h are predominantly of tetragonal structure with diffraction lines at 30.17, 35.28, 50.34, 60.14, and 63.04° on the 2-theta scale. This observation was consistent with the crystallographic card JCPDS 00-050-1089. Generally it is accepted that, for the modified zirconium oxide with oxoanions, the nature of the surface species and the crystalline

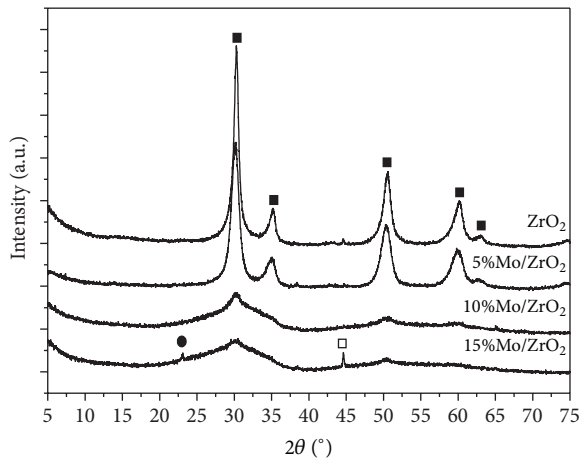

Figure 6: XRD patterns of ZrO_2 and $MoO_x{}^{y-}/ZrO_2$, (■) tetragonal ZrO_2, (□) monoclinic ZrO_2, and (●) orthorhombic MoO_3.

Table 1: Specific surface area and porous structure parameters of the synthesized materials.

Material	Surface area (m^2/g)	Pore diameter (Å)	Pore volume (cm^3/g)
ZrO_2	30	56	0.046
5%Mo/ZrO_2	118	41	0.067
10%Mo/ZrO_2	143	34	0.100
15%Mo/ZrO_2	129	38	0.089

phase of the support depend on the oxoanions loading [32]. It can be seen in Figure 6 that the molybdenum content strongly influences the crystallinity of the samples. An increase in molybdenum content results in lowering of crystallinity, which may be attributed to the suppression of crystallite growth induced by the presence of molybdenum species. In the same way as observed previously in the literature, the molybdenum species present at zirconium oxide structure were able to stabilize the tetragonal phase and promote the resistance to crystal sintering [17, 18, 33]. The absence of characteristic peaks corresponding to the molybdenum trioxide in the materials 5%Mo/ZrO_2 and 10%Mo/ZrO_2 implies that the metallic species are interacting with the zirconium oxide structure or they are highly dispersed on its surface. According to the diffractogram of the material 15%Mo/ZrO_2, a high loading of molybdenum appears to influence the appearance of the monoclinic phase, which is related to the signal at 45.21° in the 2-theta scale (JCPDS 00-072-1669) as well as the formation of MoO_3 crystals with orthorhombic structure, identified with the signal $2\theta = 23.27°$ which also appears on the X-ray pattern of the molybdenum trioxide of Figure 7 (JCPDS 00-005-0508).

3.3. Textural Properties. The nitrogen adsorption-desorption isotherms of ZrO_2 and $MoO_x{}^{y-}/ZrO_2$ samples are shown in Figures 8 and 9, together with the corresponding pore size distribution, depicted in Figures 10 and 11. The textural characterization data of the samples are included in Table 1.

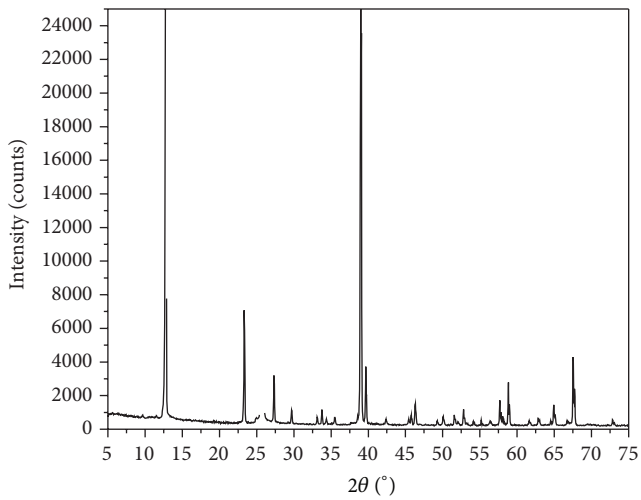

Figure 7: XRD pattern of MoO_3.

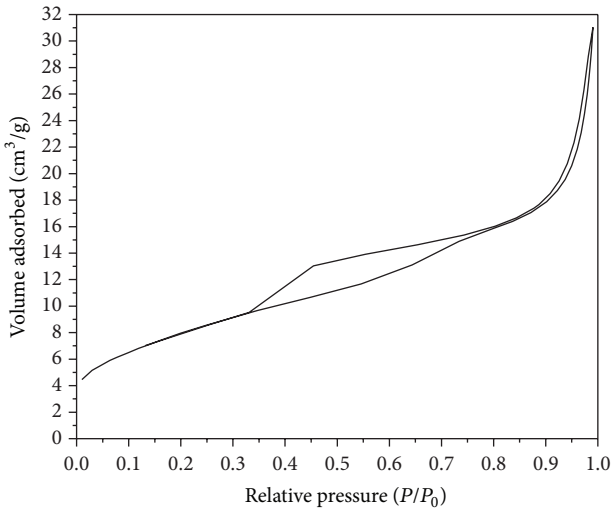

Figure 8: Nitrogen adsorption-desorption isotherm of ZrO_2.

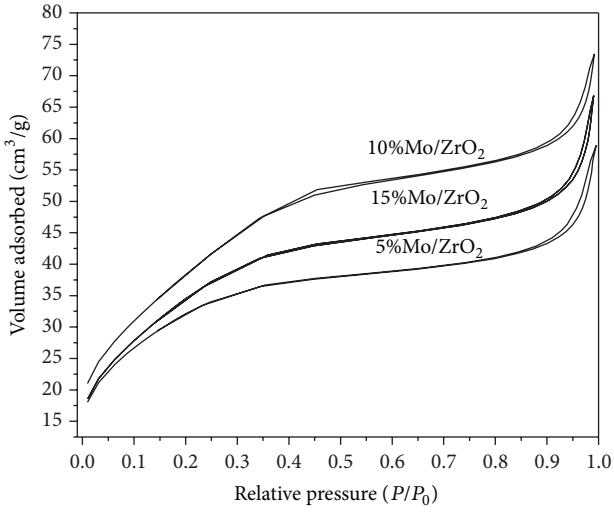

Figure 9: Nitrogen adsorption-desorption isotherms of $MoO_x{}^{y-}/ZrO_2$ materials.

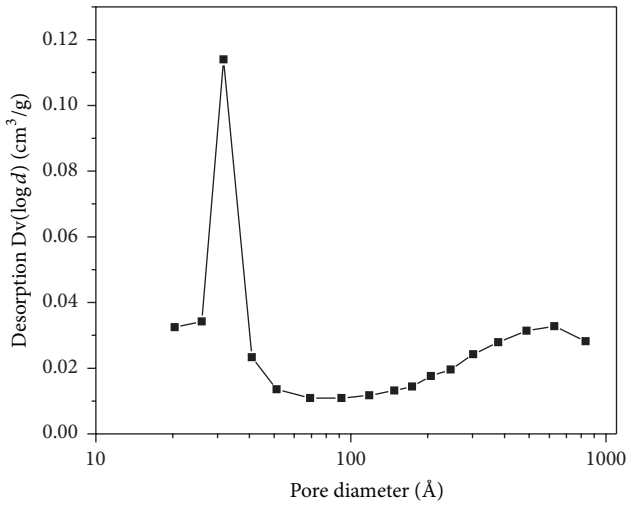

Figure 10: Pore size distribution of ZrO_2.

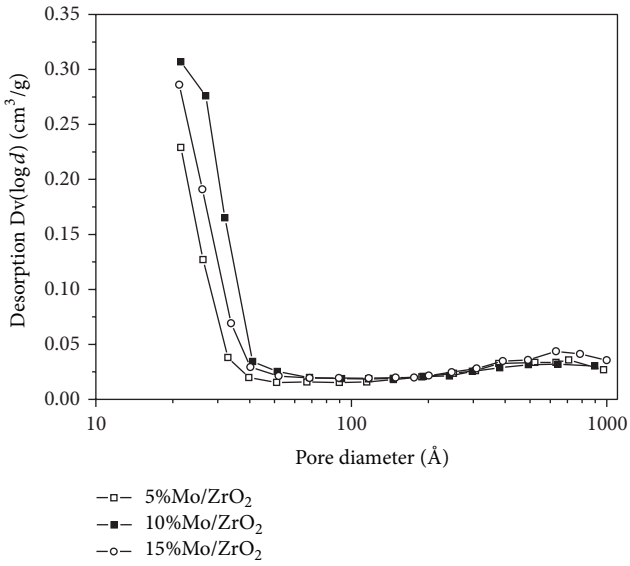

Figure 11: Pore size distribution of MoO_x^{y-}/ZrO_2 materials.

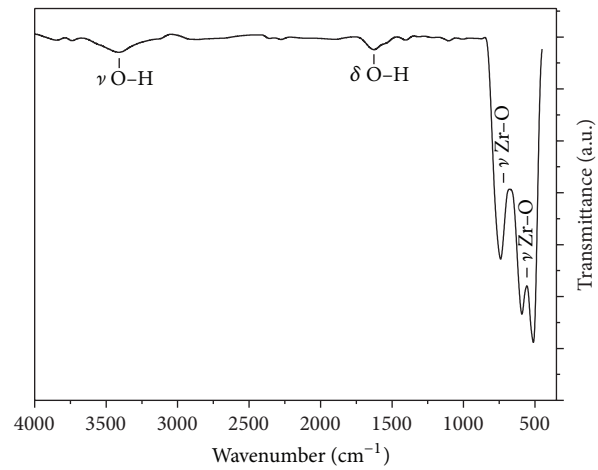

Figure 12: FT-IR spectrum of ZrO_2 sample.

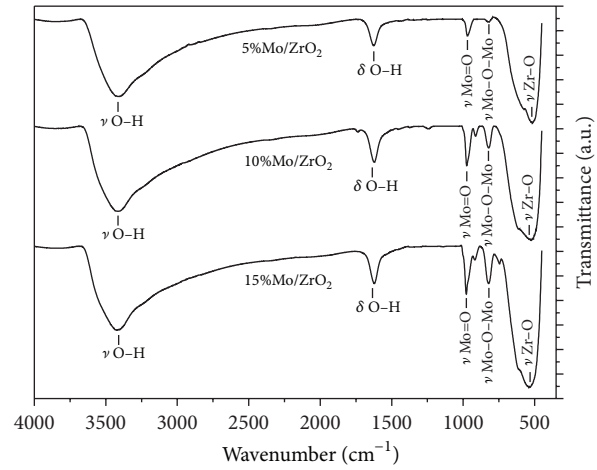

Figure 13: FT-IR spectra of MoO_x^{y-}/ZrO_2 materials.

The adsorption isotherm to pure zirconium oxide is of type IV according to Brunauer-Emmett-Teller classification typical of mesoporous materials, showing either a hysteresis cycle loop type H3; this hysteresis is usually found on solids consisting of aggregates or agglomerates of particles forming slit shaped pores. The materials modified with molybdenum developed an isotherm reflecting the presence of micro- and mesoporosity, common features of types I and IV isotherms, with reduced hysteresis loops being also observed [34, 35]. The molybdenum-modified materials show a specific surface area that exceeded up to four times the value obtained to pure zirconium oxide (30 m^2/g). With the increase of the molybdenum content from 5 to 10 wt%, the specific surface area of the material is increased from 118 to 143 m^2/g. This implies that the presence of molybdenum plays a very important role in the stability of the porous material. However, further increase in molybdenum loading to 15 wt% resulted in a decrease of the specific surface area to 129 m^2/g. Probably, when the molybdenum content increases beyond 10 wt%, pore blocking takes place due to the presence of an excessive amount of this metal and also can be related to the formation of MoO_3 surface crystals which was confirmed by X-ray diffraction. The pore size distribution of the synthesized materials has been determined by BJH method applied to desorption isotherm branch. The curves of the pore size distribution showed a bimodal distribution for pure zirconium oxide centered on the mesoporous region, changing this for MoO_x^{y-}/ZrO_2 materials to the region micro/mesoporous.

3.4. FT-IR Spectroscopy. The infrared spectra of ZrO_2 and MoO_x^{y-}/ZrO_2 samples are shown in Figures 12 and 13, respectively. A comparison of the spectra of pure zirconia with the modified samples confirms the presence of molybdate species (MoO_x^{y-}). In all modified materials broad bands were observed in the region of 3600–3400 cm^{-1} attributed to the presence of bonded hydroxyl groups to the material chemical structure as well as a band at 1639 cm^{-1} that may

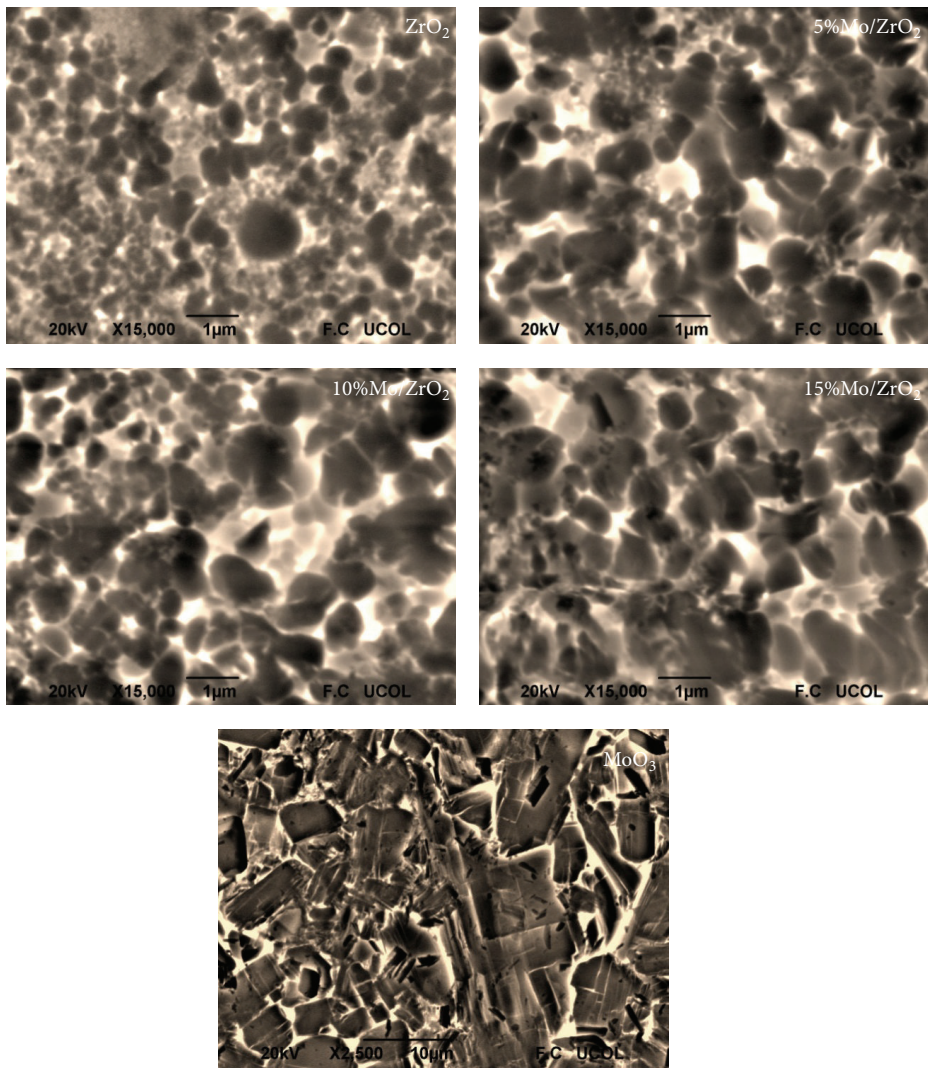

Figure 14: Scanning electron microscopy of ZrO_2, $MoO_x{}^{y-}/ZrO_2$, and MoO_3.

be attributed to the bending vibrational modes of –OH groups belonging to molecular adsorbed water [36]. No stronger peaks related to these signals were observed on pure zirconium oxide spectrum. We also speculate that these water molecules can be weakly coordinated with the molybdate species which have the ability to create acidic sites. Stronger signals at 736, 660, and 591 cm^{-1} may be assigned to stretching vibration modes of Zr–O due to the crystalline zirconium oxide [37]. The interaction of molybdenum species with the zirconium atoms was responsible for the shift at position and intensity of these signals. Another difference between pure zirconium oxide and the modified samples was found in the absorption region of 975–820 cm^{-1}. The dominant band at 975 cm^{-1} and the weak signal that appears at 912 cm^{-1} are characteristic of the stretching vibration modes of the Mo = O terminal bonds and the band at 821 cm^{-1} is associated with the vibration of Mo–O–Mo bridging bonds [38]. The increase in the intensity of these bands may be considered as a result of the molybdenum amount present in the material and also related to the increasing number of bonds.

3.5. Scanning Electron Microscopy. Figure 14 shows the scanning electron microscopy obtained with the synthesized zirconium oxides. It can be seen that the ZrO_2 exhibits spherical particles with sizes less than 1 μm and a very heterogeneous particle size distribution. The morphological characteristics of the samples are slightly modified upon molybdenum addition. The modified materials with low loadings of molybdenum (5%Mo/ZrO_2 and 10%Mo/ZrO_2) presented a better uniformity in particle size, being observed as materials consisting of spherical agglomerates, while the material 15%Mo/ZrO_2 showed that this metal loading affected the loss of spherical morphology of the material, identifying the presence of some particles with rectangular geometries, similar to that exhibited in electron microscopy of MoO_3.

4. Conclusions

The results of this work demonstrate that the molybdated zirconium oxide is a material with better thermal stability

than pure zirconium oxide. The presence and content of molybdenum retarded the transformation of zirconium hydroxide from an amorphous state to a crystalline phase of the zirconium oxide, moving this shift to higher temperatures than 420°C for the modified materials. Both synthesis variables and calcination temperature allowed developing nanocrystalline materials with tetragonal structure characteristic of ZrO_2, being the doping agent responsible for the lower crystallinity developed in the synthesized materials. The incorporation of the molybdenum into the zirconium oxide structure caused a promoting effect on its textural properties, with an increase of the specific surface area and pore volume being observed. The molybdenum-modified materials developed a specific surface area that exceeded up to four times the value obtained for pure zirconium oxide. The doping agent influenced the formation of spherical agglomerates with particle sizes smaller than 1 μm, changing the material morphology to high loadings of molybdenum. Future researches are in progress in order to study the influence of the molybdenum species interaction with the zirconium oxide structure and its effect on the acidic and catalytic properties of these materials.

Conflict of Interests

The authors declare that there is no conflict of interests regarding the publication of this paper.

References

[1] W. F. Hölderich, J. Röseler, G. Heitmann, and A. T. Liebens, "The use of zeolites in the synthesis of fine and intermediate chemicals," *Catalysis Today*, vol. 37, no. 4, pp. 353–366, 1997.

[2] G. D. Yadav and J. J. Nair, "Sulfated zirconia and its modified versions as promising catalysts for industrial processes," *Microporous and Mesoporous Materials*, vol. 33, no. 1, pp. 1–48, 1999.

[3] L. O. Alemán-Vázquez, J. L. Cano-Domínguez, E. Torres-García, and J. R. Villagómez-Ibarra, "Industrial aplication of catalytic systems for *n*-heptane isomerization," *Molecules*, vol. 16, no. 7, pp. 5916–5927, 2011.

[4] C.-C. Hwang, X.-R. Chen, S.-T. Wong, C.-L. Chen, and C.-Y. Mou, "Enhanced catalytic activity for butane isomerization with alumina-promoted tungstated mesoporous zirconia," *Applied Catalysis A: General*, vol. 323, pp. 9–17, 2007.

[5] H. Liu, G. D. Lei, and W. M. H. Sachtler, "Alkane isomerization over solid acid catalysts effects of one-dimensional micropores," *Applied Catalysis A: General*, vol. 137, no. 1, pp. 167–177, 1996.

[6] K. Tanabe, M. Misono, Y. Ono, and H. Hattori, *Studies in Surface Science and Catalysis*, Elsevier Science, Amsterdam, The Netherlands, 1990.

[7] M. L. Guevara-Franco, S. Robles-Andrade, R. García-Alamilla, G. Sandoval-Robles, and J. M. Domínguez-Esquivel, "Study of n-hexane isomerization on mixed Al_2O_3-ZrO_2/SO_4^{2-} catalysts," *Catalysis Today*, vol. 65, no. 2–4, pp. 137–141, 2001.

[8] B. M. Devassy, G. V. Shanbhag, F. Lefebvre, W. Böhringer, J. Fletcher, and S. B. Halligudi, "Zirconia-supported phosphotungstic acid as catalyst for alkylation of phenol with benzyl alcohol," *Journal of Molecular Catalysis A: Chemical*, vol. 230, no. 1-2, pp. 113–119, 2005.

[9] K. Arata, H. Matsuhashi, M. Hino, and H. Nakamura, "Synthesis of solid superacids and their activities for reactions of alkanes," *Catalysis Today*, vol. 81, no. 1, pp. 17–30, 2003.

[10] P. Moravec, J. Smolík, H. Keskinen, J. M. Mäkelä, and V. V. Levdansky, "Vapor phase synthesis of zirconia fine particles from zirconium Tetra-Tert-Butoxide," *Aerosol and Air Quality Research*, vol. 7, no. 4, pp. 563–577, 2007.

[11] J. Kaszewski, W. Łojkowski, and U. Narkiewicz, "Preparation of ZrO_2:Tb via microwave hydrothermal method," *Optica Applicata*, vol. 39, no. 4, pp. 773–779, 2009.

[12] P. Peshev, I. Stambolova, S. Vassilev et al., "Spray pyrolysis deposition of nanostructured zirconia thin films," *Materials Science and Engineering: B*, vol. 97, no. 1, pp. 106–110, 2003.

[13] J. Wenzel, "Trends in sol-gel processing: toward 2004," *Journal of Non-Crystalline Solids*, vol. 73, no. 1–3, pp. 693–699, 1985.

[14] J. Livage and C. Sanchez, "Sol-gel chemistry," *Journal of Non-Crystalline Solids*, vol. 145, pp. 11–19, 1992.

[15] A. Calafat, L. Avilán, and J. Aldana, "The influence of preparation conditions on the surface area and phase formation of MoO_3/ZrO_2 catalysts," *Applied Catalysis A: General*, vol. 201, no. 2, pp. 215–223, 2000.

[16] J. M. Hernández, L. A. Cortez, R. García, A. Castillo, G. Sandoval Robles, and L. A. García Serrano, "Synthesis and characterization of mesoporous and nano-crystalline phosphate zirconium oxides," *Journal of Alloys and Compounds*, vol. 483, no. 1-2, pp. 425–428, 2009.

[17] C.-Y. Hsu, C. R. Heimbuch, C. T. Armes, and B. C. Gates, "A highly active solid superacid catalyst for n-butane isomerization: a sulfated oxide containing iron, manganese and zirconium," *Journal of the Chemical Society, Chemical Communications*, no. 22, pp. 1645–1646, 1992.

[18] L. A. Cortez, J. M. Hernández, A. Castillo et al., "Isomerization of n-pentane with zirconium oxides dopped with borate ion," *Revista Mexicana de Ingeniería Química*, vol. 5, no. 3, pp. 321–327, 2006.

[19] V. K. Smitha, H. Stria, J. Jacob, and S. Sugunan, "Surface properties and catalytic activity of phosphate modified zirconia," *Indian Journal of Chemistry*, vol. 42, no. 2, pp. 300–304, 2003.

[20] B. M. Reddy, P. M. Sreekanth, Y. Yamada, and T. Kobayashi, "Surface characterization and catalytic activity of sulfate-, molybdate- and tungstate-promoted Al_2O_3-ZrO_2 solid acid catalysts," *Journal of Molecular Catalysis A: Chemical*, vol. 227, no. 1-2, pp. 81–89, 2005.

[21] S. Triwahyono, Z. Abdullah, and A. A. Jalil, "The effect of sulfate ion on the isomerization of n-Butane to iso-Butane," *Journal of Natural Gas Chemistry*, vol. 15, no. 4, pp. 247–252, 2006.

[22] G. Sandoval, R. Silva, J. M. Domínguez, and M. T. Ramírez, "The acidic properties characterization of zirconia-sulfonate (ZrO_2-SO_4)," *Revista Mexicana de Ingeniería Química*, vol. 3, pp. 177–180, 2004.

[23] T. Klimova, M. L. Rojas, P. Castillo, R. Cuevas, and J. Ramírez, "Characterization of Al_2O_3-ZrO_2 mixed oxide catalytic supports prepared by the sol-gel method," *Microporous and Mesoporous Materials*, vol. 20, no. 4–6, pp. 293–306, 1998.

[24] T. L. Wen, V. Hebert, S. Vilminot, and J. C. Bernier, "Preparation of nanosized yttria-stabilized zirconia powders and their characterization," *Journal of Materials Science*, vol. 26, no. 14, pp. 3787–3791, 1991.

[25] I. Atribak, B. Azambre, A. Bueno López, and A. García-García, "Effect of NO_x adsorption/desorption over ceria-zirconia catalysts on the catalytic combustion of model soot," *Applied Catalysis B: Environmental*, vol. 92, no. 1-2, pp. 126–137, 2009.

[26] J. Rack Sohn, T.-D. Kwon, and S.-B. Kim, "Characterization of zirconium sulfate supported on zirconia and activity for acid catalysis," *Bulletin of the Korean Chemical Society*, vol. 22, no. 12, pp. 1309–1315, 2001.

[27] Y. Cao, J.-C. Hu, Z.-S. Hong, J.-F. Deng, and K.-N. Fan, "Characterization of high-surface-area zirconia aerogel synthesized from combined alcohothermal and supercritical fluid drying techniques," *Catalysis Letters*, vol. 81, no. 1-2, pp. 107–112, 2002.

[28] J. A. Wang, M. A. Valenzuela, J. Salmones, A. Vázquez, A. García-Ruiz, and X. Bokhimi, "Comparative study of nanocrystalline zirconia prepared by precipitation and sol-gel methods," *Catalysis Today*, vol. 68, no. 1–3, pp. 21–30, 2001.

[29] L. Améstica, R. Quijada, and D. Villaseca, "Difusión de tecnologías, aplicaciones y desafíos del Molibdeno para la industria e investigadores a nivel nacional," in *Molibdeno: Propiedades, Aplicaciones y Mercado*, Innova, pp. 1–24, Santiago, Chile, 2010.

[30] M. Bi, H. Li, W. P. Pan, W. G. Lloyd, and B. H. Davis, "Thermal studies of $(NH_4)Cr_2O_7$, $(NH_4)_2\ WO_4$, and $(NH_4)_6Mo_7O_{24}\ .4H_2O$ on ZrO_2," *Thermochimica Acta*, vol. 284, pp. 153–160, 1996.

[31] J. R. Sohn, E. W. Chun, and Y. I. Paet, "Spectroscopic studies on ZrO_2 modified with MoO_3 and activity for acid catalysis," *Bulletin of the Korean Chemical Society*, vol. 24, no. 12, pp. 1785–1792, 2003.

[32] R. L. Martins, M. A. S. Baldanza, A. L. Alberton, S. M. R. Vasconcelos, S. F. Moya, and M. Schmal, "Effect of B and Sn on Ni catalysts supported on pure- and on WO_3/MoO_3-modified zirconias for direct CH_4 conversion to H_2," *Applied Catalysis B: Environmental*, vol. 103, no. 3-4, pp. 326–335, 2011.

[33] J. Hernández, L. García, and L. Cortez, "Physico-chemical features and catalytic activity of ZrO_2-MoO_3," *Journal of Materials Science and Engineering*, vol. 4, no. 9, pp. 1–9, 2010.

[34] K. S. W. Sing, D. H. Everett, R. A. W. Haul et al., "Reporting physisorption data for gas/solid systems with special reference to the determination of surface area and porosity," *Pure and Applied Chemistry*, vol. 57, no. 4, pp. 603–619, 1985.

[35] G. Leofanti, M. Padovan, G. Tozzola, and B. Venturelli, "Surface area and pore texture of catalysts," *Catalysis Today*, vol. 41, no. 1–3, pp. 207–219, 1998.

[36] J. Ryczkowski, "IR spectroscopy in catalysis," *Catalysis Today*, vol. 68, no. 4, pp. 263–381, 2001.

[37] J. M. H. Enríquez, L. A. G. Serrano, R. G. Alamilla, L. A. C. Lajas, and A. C. Hernández, "Síntesis, caracterización y evaluación catalítica de una ZrO_2 con fase monoclínica," *Superficies y Vacío*, vol. 22, no. 2, pp. 1–9, 2009.

[38] L. Seguin, M. Figlarz, R. Cavagnat, and J.-C. Lassègues, "Infrared and Raman spectra of MoO_3 molybdenum trioxides and $MoO_3 \cdot xH_2O$ molybdenum trioxide hydrates," *Spectrochimica Acta Part A: Molecular and Biomolecular Spectroscopy*, vol. 51, no. 8, pp. 1323–1344, 1995.